

Article

Investigating Brazilian Paintings from the 19th Century by MA-XRF

André Pimenta ¹, Valter Felix ¹, Matheus Oliveira ¹, Miguel Andrade ¹, Marcelo Oliveira ² and Renato Freitas ^{1,*}

¹ Laboratório de Instrumentação e Simulação Computacional, LISCOMP/IFRJ-CPAR, Paracambi 26600-000, Brazil; andre.pimenta@ifrj.edu.br (A.P.); valter.felix@ifrj.edu.br (V.F.); matheus.batista@ifrj.edu.br (M.O.); miguel.ao1086@gmail.com (M.A.)

² Centro Federal de Educação Tecnológica Celso Suckow da Fonseca–Campus Nova Iguaçu, Nova Iguaçu 26041-271, Brazil; marcelocefetrij@gmail.com

* Correspondence: renato.freitas@ifrj.edu.br

Abstract: In this work, four artworks dating from the 19th century by Brazilian painters Firmino Monteiro, Henrique Bernardelli, and Eliseu Visconti were analyzed by MA-XRF. Pb-L, Fe-K, and Hg-L were the main elemental maps obtained in all paintings. In the artworks of Henrique Bernardelli and Eliseu Visconti, maps of Cr-K and Co-K were also obtained. These results indicate that these Brazilian painters from the 19th century used few pigments to create their paintings, with the different hues coming mainly from ochre pigments. Using correlation image methods, no intentional mixtures of pigments made by the painters were found. These results indicate that the three painters used similar materials and techniques for preparing their pigments. These similarities are confirmed through statistical analysis by non-negative matrix factorization (NMF). In this method, it was possible to verify that the main bases of the contribution of the data registered in each artwork are the same. The analysis also revealed that one of Eliseu Visconti's paintings had an underlying painting, and another artwork by Eliseu Visconti contained a golden pigment with Cu and Zn. These results have helped art historians and conservators understand the creation process of Brazilian artists in the 19th century.

Keywords: Brazilian painting; investigation of artworks by MA-XRF; data analysis



Citation: Pimenta, A.; Felix, V.; Oliveira, M.; Andrade, M.; Oliveira, M.; Freitas, R. Investigating Brazilian Paintings from the 19th Century by MA-XRF. *Quantum Beam Sci.* **2023**, *7*, 9. <https://doi.org/10.3390/qubs7010009>

Academic Editors: Francesco Punzo and Alessandro Genoni

Received: 30 July 2022

Revised: 27 February 2023

Accepted: 3 March 2023

Published: 8 March 2023



Copyright: © 2023 by the authors. Licensee MDPI, Basel, Switzerland. This article is an open access article distributed under the terms and conditions of the Creative Commons Attribution (CC BY) license (<https://creativecommons.org/licenses/by/4.0/>).

1. Introduction

The scientific analysis of cultural heritage artifacts has expanded in recent years. The expansion of research in this field is directly related to technological development, which allowed the creation of portable instruments of different analytical techniques [1,2]. These techniques allow in situ and non-destructive analyses with great accuracy [3–6]. Among the methods applied in this field of investigation, X-ray fluorescence (XRF) stands out, as it has a simple instrumentation and can be used to study various types of cultural heritage artifacts [7–12].

XRF has great prominence among analytical techniques due to its ability to perform in situ and non-destructive analysis of elemental composition, including liquids and solids. Furthermore, advancements in technology have made portable XRF instruments increasingly accurate and easy to use, leading to its widespread adoption by researchers from diverse fields of study [13–20]. These modern instruments allow accurate and precise analysis of the elemental composition through an acquisition of a few seconds.

XRF is a well-established method based on the ionization of the atoms which make up a specific material when irradiated by a primary beam of X-rays. These ionized atoms emit photons, which contain information about the nature and abundance of the constituents elements present in the material [21,22]. As an elemental analysis technique, the characterization of pigments by XRF is based on the identification of specific key elements in the spectra associated with the color observed in the visible layer of the painting [14,23–25].

In cultural heritage, X-ray fluorescence (XRF) can be applied to various types of artifacts beyond paintings. For example, it can be used on vitreous artifacts to characterize elements directly associated with materials mixed with silica paste, which provide rigidity and color to the matrix [20,26,27]. Another application of XRF is in the analysis of metallic artifacts. XRF can be used to determine the oxidation state of the surface of alloys and the thickness of gilding layers on metallic sheets [28–31]. Ceramics also are a commonly studied artifact, and X-ray fluorescence (XRF) allows for the detection of ceramic paste and investigation of the migration routes of the producing civilization [10,32–34].

It should be noted that X-ray fluorescence (XRF) is a method that allows for elementary qualitative and quantitative analyses with wide applications in various fields of study. An example of qualitative analysis would be its use in identifying the content of certain elements, such as iron, in living organisms [35,36]. A typical application of XRF is the detection of environmental pollutants in soil [37]. These diverse applications are made possible by the instrumentation of XRF experiments, which typically do not require sample preparation and can be performed by positioning the system a few centimeters from the sample.

The Macro X-ray fluorescence scanning (MA-XRF) technique is a variation of X-ray fluorescence (XRF) and has greatly expanded the investigation of cultural heritage artifacts [38–41]. This method allows obtaining images of the elements present in the chemical matrix of the artifact. This method allows for obtaining images of the elements in the chemical matrix of the artifact and is widely used in the investigation of artworks, providing information about their conservation state and creation process [42–46]. Currently, there are commercial portable MA-XRF systems available with affordable instrumentation [47]. However, a challenge in this experiment is generating a high volume of data, which can be approached by different methods such as image correlation and statistical methods [48,49].

It should be noted that elemental mapping is a variant of XRF performed through a system composed of an X-ray tube and a detector mounted on a motorized platform, making it possible to map the elemental distribution of small areas (micro-XRF) or large surfaces (MA-XRF), as well as painting [39,40,50]. The information obtained in this study is essential in the investigation of pigments applied just below the visible painting layer of an artwork, thus revealing hidden information such as modifications made by the artist, overlapping of pigments, and restorations in the surface. In this way, the results obtained by the distribution of pigments in the pictorial layer provide a unique perspective on the artist's creative process and the history of conservation/restoration of a given painting [43,51].

There is not much literature on the use of MA-XRF to investigate Brazilian artworks. Most works that report the investigation of underlying layers of Brazilian paintings are based on X-Ray Radiography (XRRF) images. An example is described in the work of Calza et al. [52] who, when analyzing the painting "*Gioventù*" (1898) by the artist Eliseu Visconti using XRR, found traces of a complete study developed for the painting "*Recompensa de São Sebastião*" (by the same artist, dated 1897) under the surface paint layer. Another example of a Brazilian artwork studied by XRR is "*O Homem Amarelo*" (1915/1916) by artist Anita Malfatti, developed by Campos [53], whose result revealed traces of underlying layers of paintings associated with abandonment. It is essential to point out that in both cases, in addition to the radiographic images being helpful in conservation and restoration, the identification of underlying paintings are also "markers" of these artworks, as it will be difficult to reproduce them containing all these details.

In this work the MA-XRF technique was utilized to examine four 19th-century artworks by Brazilian painters: one painting each by Firmino Monteiro and Henrique Bernardelli, as well as two by Eliseu Visconti. These artists had previously had their color palettes analyzed through XRF point analysis [52,54]. However, it is fundamental to carry out more studies to deepen the knowledge of the creative process of these artworks. The results of this study are also fundamental to expanding the literature on the investigation of Brazilian artworks by MA-XRF. Through the results obtained in this study, it has been

possible to investigate the similarities between the materials used by the three painters. The results of the characterization of the palettes indicate that the painters used few pigments. To verify this similarity between the MA-XRF datasets and the materials present in the paintings, a statistical study was carried out using non-negative matrix factorization (NMF). These results contribute to the expansion of knowledge about Brazilian painters of the 19th century and support research by art historians and conservators. The work also shows a methodology to discuss similarities between MA-XRF data.

2. Materials and Methods

The analyses by MA-XRF were performed in a portable system CRONO model by Bruker, which allows scanning at once an area of $60\text{ cm} \times 45\text{ cm}$ [47]. The elemental maps were collected with the X-ray tube of Rh anode operating with a current and voltage of $200\text{ }\mu\text{A}$ and 40 kV . Collimators manufactured in brass with diameters of 1 mm and 2 mm were used in the primary beam of the tube. A silicon drift detector (SDD), model DANTE and developed by XGLab (Milano, Italy), was used for data collection, with an active area of 50 mm^2 and a resolution of 130 eV for Mn-K α energy. Spectra were collected at every 1 mm or 2 mm of the paintings for 40 ms , the scanner moving at 20 mm/s or 40 mm/s speed. With the system operating at a 10 mm distance from the analyzed object, with the 1 mm collimator, it is possible to reach a lateral resolution of 1.6 mm . The collected data cubes were analyzed using PyMca and Datamuncher [55,56]. Figure 1 shows an image of the MA-XRF instrument operating in the investigations of one of the artworks. More information about the experimental setup of the equipment used in the analyses can be seen in detail in the manuscript by Alberti et al. [47].

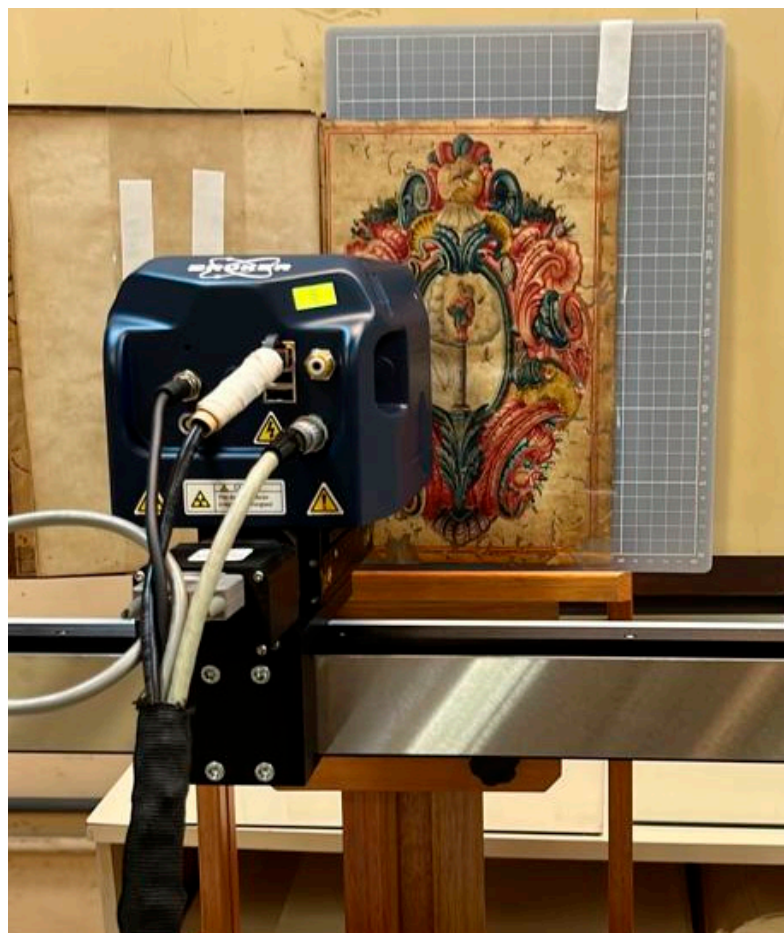


Figure 1. The module which contains the X-ray tube and detector of the MA-XRF system used in the analyses.

In the 19th century, the National School of Fine Arts was established in Brazil. Today, it is known as the School of Fine Arts at the Federal University of Rio de Janeiro. Henrique Bernardelli and Eliseu Visconti were instructors at the school, and Firmino Monteiro was a student. In this study, we analyzed the following paintings: “*Vercingetorix diante de Júlio de Cesar*” (1855–1888) by Firmino Monteiro; “*Volta do trabalho*” (1878–1886) by Henrique Bernardelli; and “*Gioventú*” (1898) by Eliseu Visconti. These three works of art from the late 19th century are part of the National Museum of Fine Arts collection in Rio de Janeiro, Brazil, where the first headquarters of the National School of Fine Arts was located. Additionally, the 1908 painting “*A poesia e o amor afastando a virtude do vício*” (1908) by Eliseu Visconti was also studied. This work is in the collection of the Municipal Theater Foundation in Rio de Janeiro, Brazil. It is the sketch for the painting on the theater’s proscenium, which Eliseu Visconti also painted. The analyzed artworks are shown in Figures 2–4.



Figure 2. Firmino Monteiro, “*Vercingetorix diante de Júlio de Cesar*”, 1855–1888, dimensions (211 cm × 161 cm), National Museum of Fine Arts/collection, Rio de Janeiro.



Figure 3. Henrique Bernardelli, “*Volta do trabalho*”, 1878–1886, dimensions (170 cm × 300 cm), National Museum of Fine Arts/collection, Rio de Janeiro.

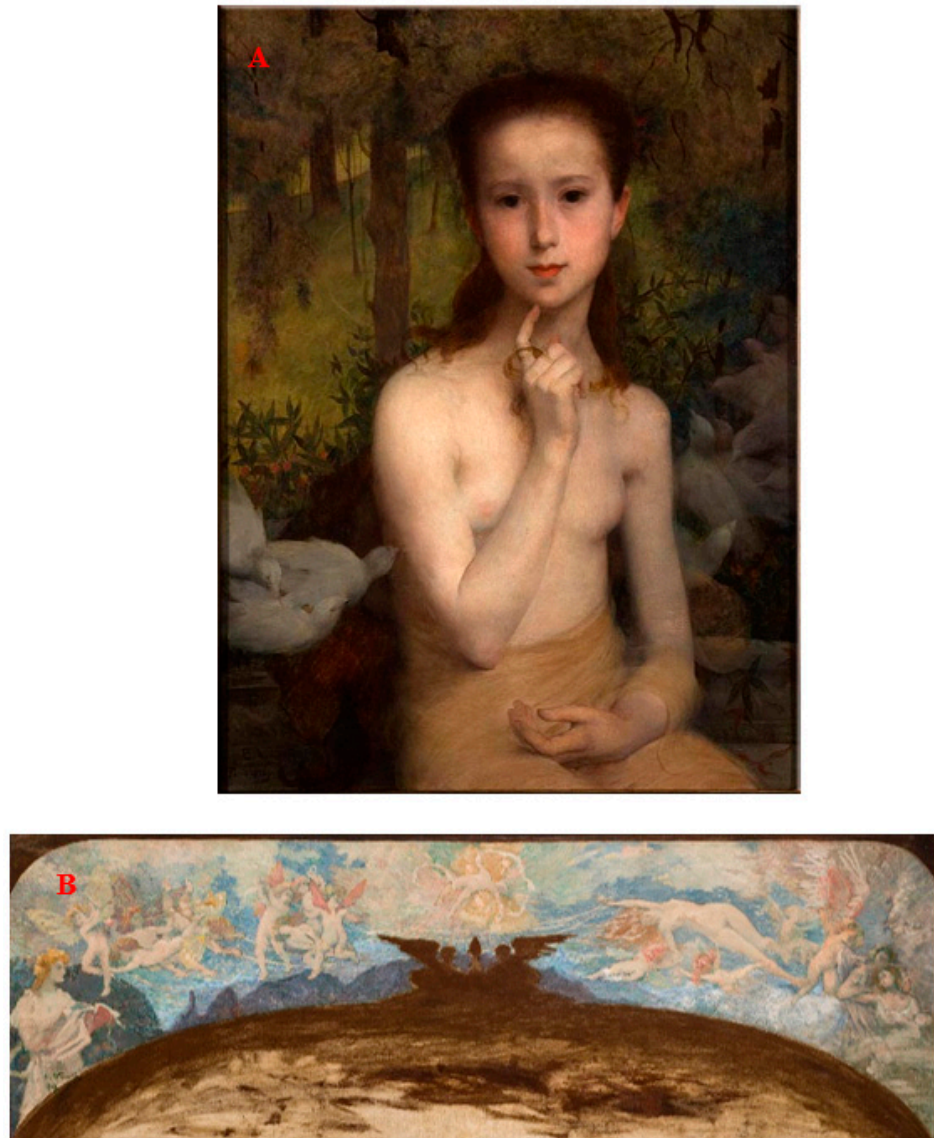


Figure 4. Eliseu Visconti, “*Gioventú*”, 1898, dimensions (65 cm × 49 cm), National Museum of Fine Arts/collection, Rio de Janeiro (A); Eliseu Visconti, “*A poesia e o amor afastando a virtude do vício*”, 1908, dimensions (170 cm × 85 cm), Municipal Theater Foundation/collection, Rio de Janeiro (B).

3. Results

The elemental maps of each data cube were constructed through evaluation by fitting the spectrum of each pixel, which forms the cubes. The fitting models were created using the sum spectra of each cube’s pixels obtained in the painting’s measurement. The fitting models were elaborated between the region of 1 keV to 16 keV using the PyMca software [55]. The evaluation by the fitting method performs a deconvolution of the spectra, allowing the capacity to obtain more precise elemental maps because the method allows verifying the contribution of each element in cases where peaks overlap—for example, in the case of K lines potassium (≈ 3.33 keV) and L lines cadmium (≈ 3.40 keV), which overlap. The method also allows deconvoluting cases of overlapping of $K\beta$ and $K\alpha$ lines. This situation is common in consecutive periodic table elements such as chromium/manganese and iron/cobalt. The elemental maps were displayed in grayscale, where the dark regions represent the smallest area integrated into the cube in the fitting process. On the other hand, the higher intensity of gray corresponds to a greater area of the elements integrated into the data cube.

Figures 5–8 shows Pb-L and Fe-K elemental maps predominant in artworks. The Pb-L maps indicate the presence of lead as the main pigment in all paintings. The lead pigments such as lead white ($(\text{PbCO}_3)_2 \cdot \text{Pb}(\text{OH})_2$) are commonly used in the paint how ground due to the drying and sealing properties [11]. This pigment is commonly found in matrices of paintings, especially after the 20th century [57]. It can be mixed with other pigments when used as ground and in the pictorial layer. Therefore, in spot XRF analyses of paintings, the presence of Pb in the spectra is common; however, one challenge is verifying whether the element comes from a superficial or underlying layer. One of the methods to investigate the position of this element in the painting would be through the differential attenuation of the characteristic X-rays, which is based on the study of the Pb-L α /Pb-L β ratios to determine whether the pigment with Pb is in the layer pictorial or ground [58–63]. However, the method requires theoretical knowledge and sometimes requires an approach that employs XRF data simulations. This verification is facilitated through elemental maps, as the use of lead as the ground is confirmed by Pb-L images, which indicate the presence of the element in the entire scanned area. However, in this analysis, the use of lead in polychrome should also be considered, especially in regions of hue tone such as flesh. Another piece of information from the Pb-L maps is the possibility of verifying ground loss. This situation can be visualized in the Pb-L images, which appear mainly in Figure 5 of Firmino Monteiro's work where black areas are seen, which indicate the absence of lead pigment. Through the Ca-K maps, it is possible to confirm these detachments of the pigment with Pb since the Ca-K images are explicitly located in these black regions of the Pb-L map.

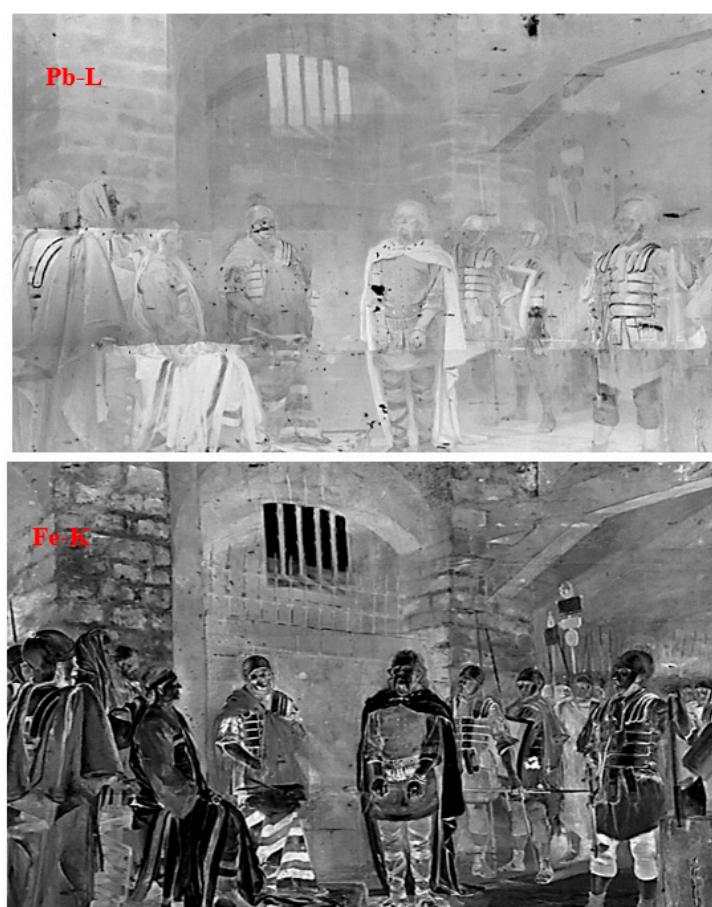


Figure 5. Pb-L and Fe-K elemental maps of painting “Vercingetorix diante de Júlio de Cesar” by Firmino Monteiro.



Figure 6. Pb-L, Fe-K, and Hg-L elemental maps of painting “Volta do trabalho” by Henrique Bernadelli. The images were obtained from a 65 cm × 45 cm region of the painting.

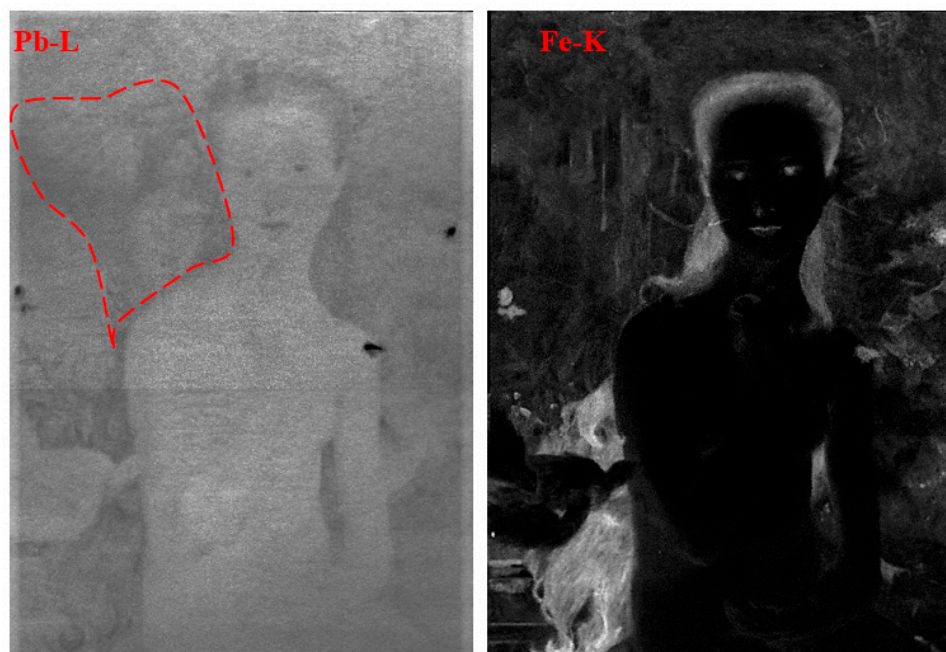


Figure 7. Pb-L and Fe-K elemental maps of painting “Gioventù” by Eliseu Visconti. On the Pb-L map, an underlying painting is shown.

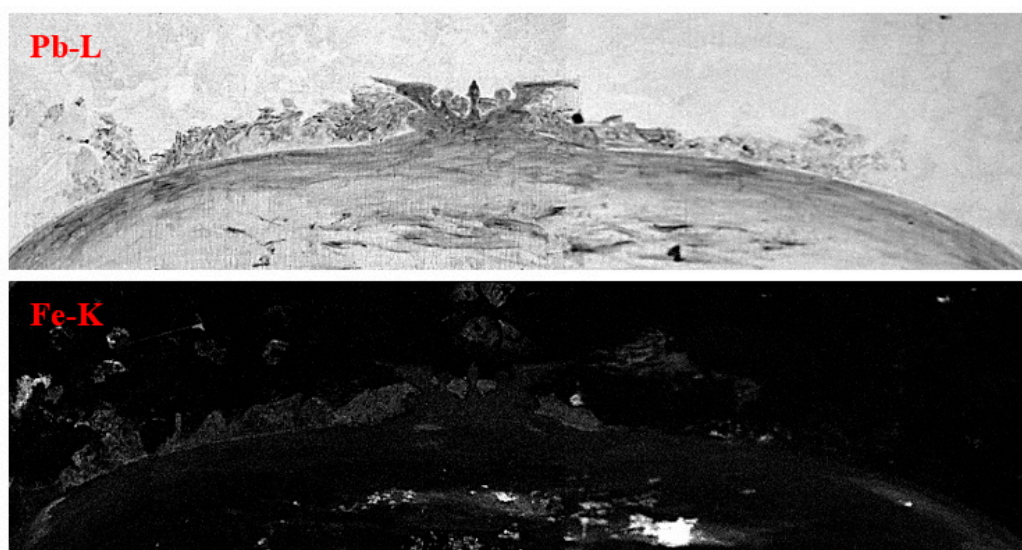


Figure 8. Elemental maps Pb-L and Fe-K of painting “*A poesia e o amor afastando a virtude do vício*” by Eliseu Visconti.

The painting “*Gioventù*” by Eliseu Visconti, a peculiarity is also seen in the Pb-L map (Figure 7). In this artwork, it is possible to visualize the sketch of another figure close to the head, indicating the reuse of the canvas. This sketch has already been evidenced in the work of Calza et al. [52], who investigated painting by radiography. The sketch is related to the artist’s painting “*Recompensa de São Sebastião*” by Eliseu Visconti, dated 1897, with dimensions 218.8 cm × 133.9 cm. This repainting indicates that Eliseu Visconti reused his canvases, a pattern seen by European painters such as Van Gogh, where analysis of artworks by MA-XRF also verified repaintings [64,65]. One hypothesis for the presence of this repainting was the possibility that Eliseu Visconti carried out an initial study for the painting “*Recompensa de São Sebastião*”, which is a methodology used by Brazilian painters such as Victor Meirelles (1832–1903), who painted artworks of significant dimensions and initially made smaller sketches of oil paintings.

The Fe-K map is present in large areas in all the paintings. For example, in Firmino Monteiro’s painting, the Fe-K map (Figure 5) appears associated with regions with red and brown hues. From the Fe-K map, it is possible to observe elements not visible in the painting (Figure 2), such as the spears in the soldiers’ hands. In Henrique Bernadelli’s artwork, the Fe-K map (Figure 6) is highlighted, especially in the regions of green hue, while in Eliseu Visconti’s artworks, Fe-K maps (Figures 7 and 8) appear in the regions of green, yellow, and blue hues. The Fe is the key element of different pigments, such as red ocher ($\text{Fe}_2\text{O}_3 + \text{clay} + \text{silica}$), yellow ocher (FeOOH), green earth ($\text{K}[(\text{Al}, \text{Fe}^{3+}), (\text{Fe}^{2+}, \text{Mg})(\text{AlSi}_3, \text{Si}_4)\text{O}_{10}(\text{OH})_2]$) and Prussian blue ($\text{Fe}_4[\text{Fe}(\text{CN})_6]_3$) [66]. These results indicate that these three Brazilian painters used Fe-based pigments as the main material in their palettes. Ocher pigments such as hematite ($\text{Fe}_2\text{O}_3 + \text{clay} + \text{silica}$) have been widely used in paintings since prehistoric times, as this pigment comes from natural sources, being an abundant type of material [67]. The green earth pigment originates from minerals such as mica, glauconite, and celadonite, which have free ions of Al, Fe, and Mg, and have a high brightness [68]. This pigment is commonly found in Roman murals in the city of Pompeii. One of the most famous sources of this pigment was near Verona, Italy [69,70]. The Prussian blue pigment is an artificial pigment that was synthesized in 1704 [71].

Another elemental map on all artworks is the Hg-L, always associated with regions of a red hue. The Hg is a key element of the vermilion pigment or the natural form of cinnabar (HgS) [11,72]. Figure 6 shows the Hg-L map of the painting “*Volta do Trabalho*” by Henrique Bernadelli. In the image, it is possible to visualize the Hg-L related to red hues such as the carnation of the personage. One of the challenges in investigating this pigment is to

determine whether it has a natural or synthetic origin, for which the presence of minerals such as quartz (SiO_2), calcite (CaCO_3), and pyrite (FeS) can be analyzed, which commonly accompany the mineral cinnabar [72]. Determining the synthetic or natural origin of HgS is essential to understand the degradation processes of this pigment, which is sensitive to light and when in its natural form, modifies the structure of the mineral cinnabar ($\alpha\text{-HgS}$) to the metacinnabar phase ($\beta\text{-HgS}$), which has a black hue [73,74]. However, to carry out this approach, it is necessary to use multiple techniques, such as Raman and Fourier transform infrared spectroscopy.

The results conclude that the palette of the three artists has significant similarities. A tool that can be employed to investigate these similarities further is multivariate statistical tools such as Principal Component Analysis [15,75]. This statistical approach can also be performed in the case of MA-XRF data, as each pixel in the image corresponds to a spectrum. In this case, the multivariate statistical approaches make it possible to obtain standards in the datasets since the number of spectra acquired in the MA-XRF measurements is superior to the different materials in the paintings. Because of this, similar spectra are repeated several times in the spectroscopic image data cubes. Furthermore, identifying these repeated data can signal patterns that bring information about the mixture of pigments adopted by the artist, which may be a characteristic of his palette, with a substantial probability of being repeated in different artworks [49,76].

$$\begin{array}{c} \text{original matrix (V)} \\ \text{data cube} \end{array} \quad \begin{array}{c} \overbrace{\left(\begin{array}{ccc} \cdots & & \\ \vdots & \ddots & \vdots \\ & & \cdots \end{array} \right)}^{n \times p} \\ \\ \end{array} = \underbrace{\begin{array}{c} \left(\begin{array}{ccc} \cdots & & \\ \vdots & \ddots & \vdots \\ & & \cdots \end{array} \right) \\ \text{bases (X)} \end{array}}_{n \times k} \times \begin{array}{c} \text{intensities and pixels} \\ \text{for each base (Y)} \end{array} \quad \begin{array}{c} \overbrace{\left(\begin{array}{ccc} \cdots & & \\ \vdots & \ddots & \vdots \\ & & \cdots \end{array} \right)}^{k \times p} \\ \\ \end{array} \quad (1)$$

To investigate the patterns repeated in the painting data cube, multivariate statistical analysis by non-negative matrix factorization (NMF) were performed. The theoretical background of this method is based on factoring data cube matrix ($V_{n \times p}$) into two non-negative matrices in this analysis. Being a call of the base ($X_{n \times k}$) will contain information on the most relevant elements for that group, which are the most repeated spectra in the datasets. Another matrix ($Y_{k \times p}$) already contains information on intensities and pixels for each base [49,77]. Equation (1) illustrates the factoring process involving these matrices.

The NMF, such as Principal Component Analysis (PCA), indicates similar groups in the datasets. In the case of images, the bases constitute groups of the combination of elements, which occur more frequently in the formation of images. However, the NMF differs from the PCA because the base information does not have negative values. In this work, the NMF process was carried out through routines available in the PyMca software [55]. The NMF method tool from PyMca was applied with the analysis range limited to 0 keV to 20 keV. The software was selected to conduct the NMF process, factoring in 10 different bases. The results show that the first base of each dataset of MA-XRF of the paintings represents more than 90% of the data variance. This suggests that the first component has a significant impact on the representation of each painting's MA-XRF dataset. Figure 9 shows the first base of the data cube of each painting. It is possible to verify that the combination of Fe-K and Pb-L elements form them in all bases. It is worth noting that the other components, accounting for the remaining 10% of the variance, also always include a combination of Fe and Pb with other elements. This result confirms the prevalence of Fe- and Pb-based pigments in the artwork of these three Brazilian painters in the 19th century, confirming the similarity in the painters' pigment palette.

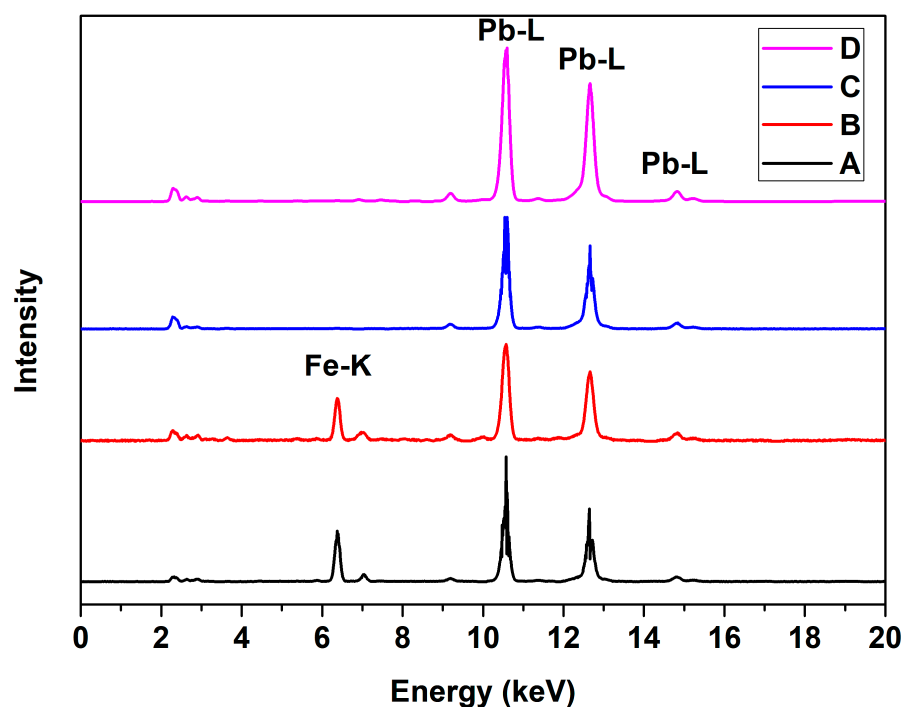


Figure 9. First base obtained in the analysis by NMF of the MA-XRF data of the paintings. Firmino Monteiro (A); Henrique Bernadelli (B); “Gioventù” from Eliseu Visconti (C); “A poesia e o amor afastando a virtude do vício” from Eliseu Visconti (D).

Eliseu Visconti’s paintings presented the most variety of bases, with combinations of elements beyond Fe and Pb. The presence of pigments with other elements had already been visualized by MA-XRF maps, where images of Cr-K, Co-K, Cu-K, and Zn-K were obtained. These elements can be correlated to pigments such as green chromium oxide (Cr_2O_3), cobalt blue ($\text{CoO} \cdot \text{Al}_2\text{O}_3$), or cobalt green ($\text{CoO} \cdot n\text{ZnO}$) when associated with Zn and the blue pigment azurite ($\text{Cu}_3(\text{CO}_3)_2(\text{OH})_2$). These type of pigments were found in the artwork of Calza et al. [54] when investigating paintings by different Brazilian painters of the 19th century. However, it is essential to point out that these maps appear in isolated regions, and Pb-L, Fe-K, and Hg-L maps are predominating in the paintings.

In the painting “A poesia e o amor afastando a virtude do vício” by Eliseu Visconti, a golden region of the painting (Figure 4B) stands out, where maps of Cu-K and Zn-K are visible. To determine a correlation between these maps, scatterplots were created by correlating pixel intensities. These scatterplots are developed by correlating the intensity of the same pixel in two images. Each point on the graph corresponds to the pixel’s intensity in the Cu-K and Zn-K maps. In this work, the Cu-K vs. Zn-K scatterplot (Figure 10) was created using routines from Datamuncher software [56]. In the Cu-K vs. Zn-K scatterplot, a linear trend region is seen, which indicates the presence of brass in the pigments [78]. The correlation image in cyan color highlights the linear trend points corresponding to the golden region of the painting, indicating that this hue is a result of the presence of brass pigment. Therefore, this golden hue is due to the presence of the pigment with brass. Another region of Zn-K without correlation is seen in the graph, indicating probable areas of restoration carried out with zinc white (ZnO) pigment. In all paintings, Zn-K maps were obtained in isolated regions, which can be associated with retouching regions. These correlation tests were performed on MA-XRF datasets of all artworks, but no relevant scatterplots were obtained, which referred to the mixed pigments. The absence of these image correlations reinforces the use of few pigments in the artists’ artworks.

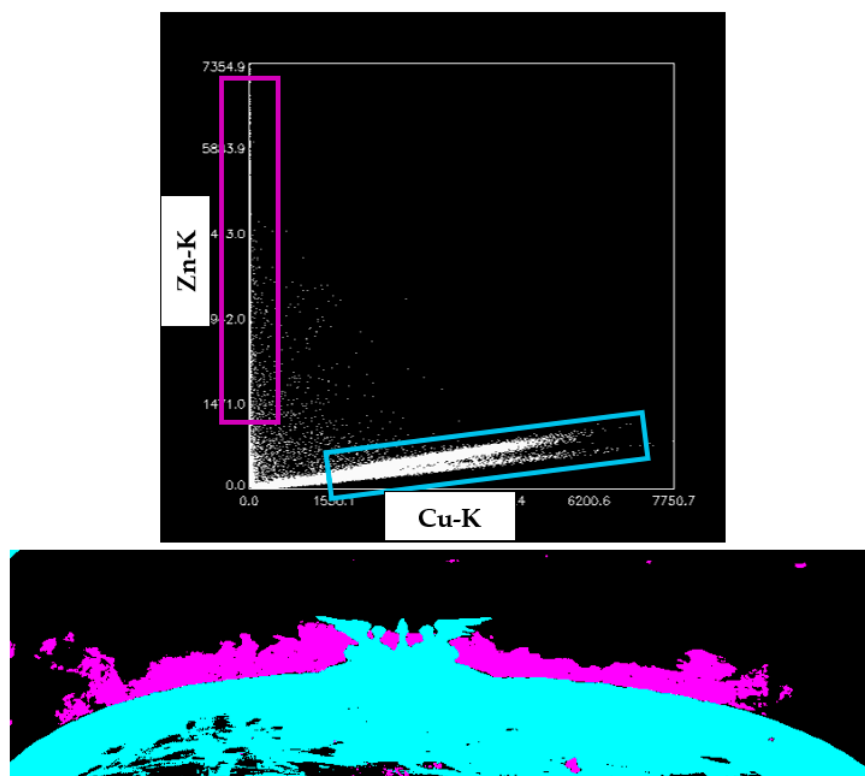


Figure 10. Scatter plot Cu-K vs. Zn-K of painting “*A poesia e o amor afastando a virtude do vício*” by Eliseu Visconti.

4. Discussion

From the results, it was possible to verify that the Brazilian painters of the 19th century Firmino Monteiro, Henrique Bernadelli, and Eliseu Visconti had limited access to materials. The base palette is mainly composed of iron-based pigments, such as red ochre ($\text{Fe}_2\text{O}_3 + \text{clay} + \text{silica}$), yellow ochre (FeOOH), Prussian blue ($\text{Fe}_4[\text{Fe}(\text{CN})_6]_3$), and earth green ($\text{K}[(\text{Al}, \text{Fe}^{3+}), (\text{Fe}^{2+}, \text{Mg})(\text{AlSi}_3, \text{Si}_4)\text{O}_{10}(\text{OH})_2]$). Therefore, the hue variations seen in the artworks were likely achieved by mixing pigments.

In Eliseu Visconti’s paintings, different pigments in some regions were observed. In the painting “*A poesia e o amor afastando a virtude do vício*”, the use of a pigment containing brass was characterized. In the “*Gioventù*” painting, a sketch of another famous work by Eliseu Visconti was also seen. It is noteworthy that Eliseu Visconti frequently traveled to Europe, where he had exchanges with other painters and access to various materials. This exchange with European painters explains the use of materials other than Pb and Fe pigments in his works.

Through this study, it was possible to gain a better understanding of the materials used by Brazilian painters of the 19th century. The results of this work are significant in terms of expanding knowledge of the materials used by Brazilian painters. Additionally, this information will assist art historians and conservators in comprehending the creative process of Brazilian painters from the 19th century. It is crucial to highlight that Henrique Bernadelli and Eliseu Visconti were instructors at the National School of Fine Arts in Brazil and had a significant impact on Brazilian painters of the 20th century. The results of this study will be useful for future studies on Brazilian painters of the 20th century. The outcomes of this study will also benefit future researchers who aim to study Brazilian paintings from the 19th century using other analytical techniques such as Fourier Transform Infrared Spectroscopy (FTIR).

Regarding the data analysis conducted in this study, it highlights the importance of utilizing methods such as statistical analysis and image correlation to gain further insights into the MA-XRF data. For instance, the use of NMF revealed that Pb and Fe were the

elements with the most substantial contribution to the matrix of the paintings. NMF also confirmed the similarity of the pigments used by different painters in their artworks. Image correlation, which generates a scatterplot and correlation image, clearly demonstrated that the golden region of the painting “*A poesia e o amor afastando a virtude do vício*” was created using a brass pigment. It is worth mentioning that image correlation tests were performed on data from all paintings, but no noteworthy results were obtained. The need to carry out approaches to investigate patterns in MA-XRF datasets is highlighted. In addition to reducing the analysis time, this methodology allows for a more straightforward verification of the materials, which are most repeated in the datasets.

The results present in this one are also essential to understand the exchange between Brazilian painters of the 19th century and European painters. It is noteworthy that this exchange was also common during the 20th century, where Brazilian painters from the modernist period, such as Tarsila do Amaral made regular exchanges in Europe. Therefore, the results of this study open the possibility of investigating the European artistic schools which most influenced Brazilian painters of the 19th century. The presence of few pigments on the painters’ palettes is an indication that in Brazil in this period there was no local production of pigments, which makes this material expensive to acquire.

It highlights the need to deepen the knowledge of these paintings, which can be accomplished by applying other analysis techniques, such as microsamples analyses by spectroscopic methods. In these analyses, it would be possible to determine, for example, the molecular composition of pigments. In this case, the images by MA-XRF make it possible to screen which regions need to be deepened by microanalyses. For example, in the case of the “*Vercingetorix in front of Júlio de Cesar*” by Firmino Monteiro, it would be interesting to study the restored regions. In the painting “*A poesia e o amor afastando a virtude do vício*” by Eliseu Visconti, it would be possible to investigate the pigment composed of Cu and Zn and its influences on the environment, which can lead to the phenomena of degradation of pigments.

Author Contributions: Conceptualization, A.P., V.F. and R.F.; methodology, A.P., V.F. and R.F.; software, R.F., M.O. (Matheus Oliveira) and M.A.; validation, A.P., V.F., M.O. (Marcelo Oliveira) and R.F.; formal analysis, A.P., V.F., M.O. (Matheus Oliveira), M.A., M.O. (Marcelo Oliveira) and R.F.; investigation, A.P., V.F., M.O. (Matheus Oliveira), M.A., M.O. (Marcelo Oliveira) and R.F.; resources, A.P., V.F. and R.F.; data curation, A.P., V.F. and R.F.; writing—original draft preparation, A.P. and R.F.; writing—review and editing, A.P., V.F., M.O. (Matheus Oliveira), M.A., M.O. (Marcelo Oliveira) and R.F.; visualization, A.P., V.F. and R.F.; supervision, R.F.; project administration, A.P.; funding acquisition, R.F. All authors have read and agreed to the published version of the manuscript.

Funding: This research was funded by Foundation for Research Support of the State of Rio de Janeiro (FAPERJ—Fundação de Amparo à Pesquisa do Estado do Rio de Janeiro, grant number E-26/210.143/2022, E-26/290.023/2021, E-26/290.066/2018, E-26/204.040/2021 and E-26/202.672/2018 and “The APC was funded by MDPI”.

Data Availability Statement: Not applicable.

Acknowledgments: We thank IFRJ’s Pro-rectory of Research, Innovation and Graduate Studies (PROPPI—Pró-reitoria de Pesquisa, Inovação e Pós-Graduação) for its financial support from grant number 01/2021. We also thank the Foundation for Research Support of the State of Rio de Janeiro (FAPERJ—Fundação de Amparo à Pesquisa do Estado do Rio de Janeiro), for their financial support through project grant numbers E-26/210.143/2022, E-26/290.023/2021, E-26/290.066/2018, E-26/204.040/2021 and E-26/202.672/2018. We thank the National Council for Scientific and Technological Development (CNPq—Conselho Nacional de Pesquisa) for its financial support grant number 422557/2021-8. We thank staff from Museu Nacional de Belas Artes, Rio de Janeiro e Fundação Teatro Municipal, Rio de Janeiro.

Conflicts of Interest: The authors declare no conflict of interest.

References

1. Miliani, C.; Rosi, F.; Brunetti, B.G.; Sgamellotti, A. In Situ Noninvasive Study of Artworks: The MOLAB Multitechnique Approach. *Acc. Chem. Res.* **2010**, *43*, 728–738. [\[CrossRef\]](#)
2. Brunetti, B.; Miliani, C.; Rosi, F.; Doherty, B.; Monico, L.; Romani, A.; Sgamellotti, A. Non-invasive investigations of paintings by portable instrumentation: The MOLAB experience. *Top. Curr. Chem.* **2016**, *374*, 10. [\[CrossRef\]](#)
3. Ford, T.; Rizzo, A.; Hendriks, E.; Frøysaker, T.; Caruso, F. A non-invasive screening study of varnishes applied to three paintings by Edvard Munch using portable diffuse reflectance infrared Fourier transform spectroscopy (DRIFTS). *Herit. Sci.* **2019**, *7*, 84. [\[CrossRef\]](#)
4. Monico, L.; Cartechini, L.; Rosi, F.; Chieli, A.; Grazia, C.; De Meyer, S.; Nuyts, G.; Vanmeert, F.; Janssens, K.; Cotte, M.; et al. Probing the chemistry of CdS paints in The Scream by in situ noninvasive spectroscopies and synchrotron radiation x-ray techniques. *Sci. Adv.* **2020**, *6*, eaay3514. [\[CrossRef\]](#) [\[PubMed\]](#)
5. Vagnini, M.; Malagodi, M.; Gabrieli, F.; Azzarelli, M.; Nucera, F.; Daveri, A. An Integrated and Analytical Approach to Study of Mural Paintings: The Case of “Lo Spagna” in Spoleto. *Int. J. Conserv. Sci.* **2018**, *9*, 401–412.
6. Vagnini, M.; Gabrieli, F.; Daveri, A.; Sali, D. Handheld new technology Raman and portable FT-IR spectrometers as complementary tools for the in situ identification of organic materials in modern art. *Spectrochim. Acta Part A Mol. Biomol. Spectrosc.* **2017**, *176*, 174–182. [\[CrossRef\]](#)
7. Freitas, R.P.; Coelho, F.A.; Felix, V.S.; Pereira, M.O.; de Souza, M.A.T.; Anjos, M.J. Analysis of 19th century ceramic fragments excavated from Pirenópolis (Goiás, Brazil) using FT-IR, Raman, XRF and SEM. *Spectrochim. Acta Part A Mol. Biomol. Spectrosc.* **2018**, *193*, 432–439. [\[CrossRef\]](#) [\[PubMed\]](#)
8. Sanches, F.A.C.R.d.A.; Nardes, R.C.; Filho, H.S.G.; dos Santos, R.S.; de Araújo, O.M.O.; Machado, A.S.; Calgam, T.; Bueno, R.; Canellas, C.; Gonçalves, E.A.S.; et al. Characterization of a sacred statuette replica of “Nossa Senhora da Conceição Aparecida” using X-ray spectroscopy techniques. *Radiat. Phys. Chem.* **2020**, *167*, 108266. [\[CrossRef\]](#)
9. Freitas, R.P.; Ribeiro, I.M.; Calza, C.; Oliveira, A.L.; Felix, V.S.; Ferreira, D.S.; Pimenta, A.R.; Pereira, R.V.; Pereira, M.O.; Lopes, R.T. Analysis of a Brazilian baroque sculpture using Raman spectroscopy and FT-IR. *Spectrochim. Acta Part A Mol. Biomol. Spectrosc.* **2016**, *154*, 67–71. [\[CrossRef\]](#)
10. Freitas, R.P.; Calza, C.; Lima, T.A.; Rabello, A.; Lopes, R.T. EDXRF and multivariate statistical analysis of fragments from Marajoara ceramics. *X-ray Spectrom.* **2010**, *39*, 307–310. [\[CrossRef\]](#)
11. Felix, V.S.; Mello, U.L.; Pereira, M.O.; Oliveira, A.L.; Ferreira, D.S.; Carvalho, C.S.; Silva, F.L.; Pimenta, A.R.; Diniz, M.G.; Freitas, R.P. Analysis of a European cupboard by XRF, Raman and FT-IR. *Radiat. Phys. Chem.* **2018**, *151*, 198–204. [\[CrossRef\]](#)
12. Ribeiro, I.M.N.; Freitas, R.P.; Calza, C.; Oliveira, A.L.C.; Felix, V.S.; Ferreira, D.S.; Batista, R.T.; Gonçalves, E.A.S.; Pereira, M.O.; Brito, P.C.L.; et al. Analysis by raman spectroscopy and XRF of glass beads from excavations in the harbor area of rio de janeiro, Brazil. *Vib. Spectrosc.* **2016**, *87*, 111–115. [\[CrossRef\]](#)
13. Vanhoof, C.; Bacon, J.R.; Ellis, A.T.; Fittschen, U.E.A.; Vincze, L. 2019 atomic spectrometry update—A review of advances in X-ray fluorescence spectrometry and its special applications. *J. Anal. At. Spectrom.* **2019**, *34*, 1750–1767. [\[CrossRef\]](#)
14. Molari, R.; Appoloni, C.R. Pigment analysis in four paintings by Vincent van Gogh by portable X-ray fluorescence (pXRF). *Radiat. Phys. Chem.* **2021**, *181*, 109336. [\[CrossRef\]](#)
15. de Queiroz Baddini, A.L.; de Paula Santos, J.L.V.; Tavares, R.R.; de Paula, L.S.; da Costa Araújo Filho, H.; Freitas, R.P. PLS-DA and data fusion of visible Reflectance, XRF and FTIR spectroscopy in the classification of mixed historical pigments. *Spectrochim. Acta Part A Mol. Biomol. Spectrosc.* **2022**, *265*, 120384. [\[CrossRef\]](#)
16. Scialla, E.; Improda, P.; Brocchieri, J.; Cardinali, M.; Cerasuolo, A.; Rullo, A.; Zezza, A.; Sabbarese, C. Study of ‘Cona degli Ordini’ by Colantonio with IR and XRF Analyses. *Heritage* **2023**, *6*, 1785–1803. [\[CrossRef\]](#)
17. Klisińska-Kopacz, A.; Frączek, P.; Obarzanowski, M.; Czop, J. Non-Invasive Study of Pigment Palette Used by Olga Boznańska Investigated with Analytical Imaging, XRF, and FTIR Spectroscopy. *Heritage* **2023**, *6*, 1429–1443. [\[CrossRef\]](#)
18. Andrade, R.; Silva, S.H.G.; Benedet, L.; de Araújo, E.F.; Carneiro, M.A.C.; Curi, N. A Proximal Sensor-Based Approach for Clean, Fast, and Accurate Assessment of the *Eucalyptus* spp. Nutritional Status and Differentiation of Clones. *Plants* **2023**, *12*, 561. [\[CrossRef\]](#)
19. Zhou, S.; Wang, J.; Wang, W.; Liao, S. Evaluation of Portable X-ray Fluorescence Analysis and Its Applicability As a Tool in Geochemical Exploration. *Minerals* **2023**, *13*, 166. [\[CrossRef\]](#)
20. Yatsuk, O.; Ferretti, M.; Gorghinian, A.; Fiocco, G.; Malagodi, M.; Agostino, A.; Gulmini, M. Data from Multiple Portable XRF Units and Their Significance for Ancient Glass Studies. *Molecules* **2022**, *27*, 6068. [\[CrossRef\]](#)
21. Janssens, K.H.A.; Adams, F.; Rindby, A. *Microscopic X-ray Fluorescence Analysis*; Wiley Chichester: Chichester, UK, 2000.
22. Arai, T.; Langhoff, N.; Simionovici, A.; Arkadiev, V.; Knüpfer, W.; Cechák, T.; Leonhardt, J.; Chavanne, J.; Erko, A.; Bjeoumikhov, A.; et al. *Handbook of Practical X-ray Fluorescence Analysis*; Springer: Berlin/Heidelberg, Germany, 2006. [\[CrossRef\]](#)
23. Campos, P.H.O.V.; Kajijiya, E.A.M.; Rizzutto, M.A.; Neiva, A.C.; Pinto, H.P.F.; Almeida, P.A.D. X-ray fluorescence and imaging analyses of paintings by the Brazilian artist Oscar Pereira Da Silva. *Radiat. Phys. Chem.* **2014**, *95*, 362–367. [\[CrossRef\]](#)
24. Appoloni, C.R.; Blonski, M.S.; Parreira, P.S.; Souza, L.A.C. Study of the pigments elementary chemical composition of a painting in process of attribution to Gainsborough employing a portable X-rays fluorescence system. *Nucl. Instrum. Methods Phys. Res. Sect. A Accel. Spectrometers Detect. Assoc. Equip.* **2007**, *580*, 710–713. [\[CrossRef\]](#)

25. Neiva, A.C.; Marcondes, M.A.; Pinto, H.P.F.; Almeida, P.A.D. Analysis of photographs and photo-paintings by energy-dispersive X-ray fluorescence spectroscopy. *Radiat. Phys. Chem.* **2014**, *95*, 378–380. [\[CrossRef\]](#)
26. Colomban, P.; Simsek Franci, G.; Burlot, J.; Gallet, X.; Zhao, B.; Clais, J.-B. Non-Invasive On-Site pXRF Analysis of Coloring Agents, Marks and Enamels of Qing Imperial and Non-Imperial Porcelain. *Ceramics* **2023**, *6*, 447–474. [\[CrossRef\]](#)
27. Burlot, J.; Gallet, X.; Simsek Franci, G.; Bellot-Gurlet, L.; Colomban, P. Non-Invasive On-Site pXRF Analysis of Coloring Agents of Under- and Over-Glazes: Variability and Representativity of Measurements on Porcelain. *Colorants* **2023**, *2*, 42–57. [\[CrossRef\]](#)
28. Trojek, T.; Trojková, D. Uncertainty of Quantitative X-ray Fluorescence Micro-Analysis of Metallic Artifacts Caused by Their Curved Shapes. *Materials* **2023**, *16*, 1133. [\[CrossRef\]](#)
29. Mathoho, E.N.; Nyamushosho, R.T.; Chirikure, S. Archaeometallurgical Explorations of Bloomery Iron Smelting at Mutoti 2, an Early Iron Age Site in Venda, Northern South Africa. *Metals* **2023**, *13*, 269. [\[CrossRef\]](#)
30. Felix, V.S.; Pereira, M.O.; Freitas, R.P.; Aranha, P.J.M.; Heringer, P.C.S.; Anjos, M.J.; Lopes, R.T. Analysis of silver coins from colonial Brazil by hand held XRF and micro-XRF. *Appl. Radiat. Isot.* **2020**, *166*, 109409. [\[CrossRef\]](#)
31. Cesareo, R.; Franco Jordan, R.; Fernandez, A.; Bustamante, A.; Fabian, J.; del Pilar Zambrano, S.; Azeredo, S.; Lopes, R.T.; Ingo, G.M.; Riccucci, C.; et al. Analysis of the spectacular gold and silver from the Moche tomb “Señora de Cao”. *X-ray Spectrom.* **2016**, *45*, 138–154. [\[CrossRef\]](#)
32. Kulkova, M.A.; Kashuba, M.T.; Kulkov, A.M.; Vetrova, M.N. Pottery of Early Iron Age from the Glinjeni II-La Şant (North-Western Pontic Sea Region): Composition, Technology and Raw Material Sources. *Heritage* **2021**, *4*, 2853–2875. [\[CrossRef\]](#)
33. Zhushchikhovskaya, I.S.; Buravlev, I.Y. Ancient Ceramic Casting Molds from the Southern Russian Far East: Identification of Alloy Traces via Application of Nondestructive SEM-EDS and pXRF Methods. *Heritage* **2021**, *4*, 2643–2667. [\[CrossRef\]](#)
34. Demirsar Arli, B.; Simsek Franci, G.; Kaya, S.; Arli, H.; Colomban, P. Portable X-ray Fluorescence (p-XRF) Uncertainty Estimation for Glazed Ceramic Analysis: Case of Iznik Tiles. *Heritage* **2020**, *3*, 1302–1329. [\[CrossRef\]](#)
35. Dao, E.; Zeller, M.P.; Wainman, B.C.; Farquharson, M.J. Feasibility of the use of a handheld XRF analyzer to measure skin iron to monitor iron levels in critical organs. *J. Trace Elem. Med. Biol.* **2018**, *50*, 305–311. [\[CrossRef\]](#) [\[PubMed\]](#)
36. Jyothsna, S.; Manjula, G.; Chandar Rao, P.; Mahesh Kumar, A.; Sammaiah, D.; Nageswara Rao, A.S. Computational screening of trace elemental concentrations in *Hemidesmus indicus* L. A potential herbal plant used against skin diseases by ED-XRF-Technique. *Mater. Today Proc.* **2021**, *46*, 2221–2225. [\[CrossRef\]](#)
37. Mera, M.F.; Rubio, M.; Pérez, C.A.; Cazón, S.; Merlo, M.; Muñoz, S.E. SR induced micro-XRF for studying the spatial distribution of Pb in plants used for soil phytoremediation. *Radiat. Phys. Chem.* **2019**, *154*, 69–73. [\[CrossRef\]](#)
38. Santos, H.C.; Caliri, C.; Pappalardo, L.; Catalano, R.; Orlando, A.; Rizzo, F.; Romano, F.P. Identification of forgeries in historical enamels by combining the non-destructive scanning XRF imaging and alpha-PIXE portable techniques. *Microchem. J.* **2016**, *124*, 241–246. [\[CrossRef\]](#)
39. Romano, F.P.; Caliri, C.; Nicotra, P.; Di Martino, S.; Pappalardo, L.; Rizzo, F.; Santos, H.C. Real-time elemental imaging of large dimension paintings with a novel mobile macro X-ray fluorescence (MA-XRF) scanning technique. *J. Anal. At. Spectrom.* **2017**, *32*, 773–781. [\[CrossRef\]](#)
40. Alfeld, M.; Pedroso, J.V.; van Eikema Hommes, M.; Van der Snickt, G.; Tauber, G.; Blaas, J.; Haschke, M.; Erler, K.; Dik, J.; Janssens, K. A mobile instrument for in situ scanning macro-XRF investigation of historical paintings. *J. Anal. At. Spectrom.* **2013**, *28*, 760–767. [\[CrossRef\]](#)
41. Alfeld, M.; de Viguere, L. Recent developments in spectroscopic imaging techniques for historical paintings—A review. *Spectrochim. Acta Part B At. Spectrosc.* **2017**, *136*, 81–105. [\[CrossRef\]](#)
42. Van der Snickt, G.; Legrand, S.; Slama, I.; Van Zuien, E.; Gruber, G.; Van der Stighelen, K.; Klaassen, L.; Oberthaler, E.; Janssens, K. In situ macro X-ray fluorescence (MA-XRF) scanning as a non-invasive tool to probe for subsurface modifications in paintings by P.P. Rubens. *Microchem. J.* **2018**, *138*, 238–245. [\[CrossRef\]](#)
43. Legrand, S.; Vanmeert, F.; Van der Snickt, G.; Alfeld, M.; De Nolf, W.; Dik, J.; Janssens, K. Examination of historical paintings by state-of-the-art hyperspectral imaging methods: From scanning infra-red spectroscopy to computed X-ray laminography. *Herit. Sci.* **2014**, *2*, 13. [\[CrossRef\]](#)
44. Van der Snickt, G.; Legrand, S.; Caen, J.; Vanmeert, F.; Alfeld, M.; Janssens, K. Chemical imaging of stained-glass windows by means of macro X-ray fluorescence (MA-XRF) scanning. *Microchem. J.* **2016**, *124*, 615–622. [\[CrossRef\]](#)
45. Janssens, K.; Alfeld, M.; der Snickt, G.; De Nolf, W.; Vanmeert, F.; Radepon, M.; Monico, L.; Dik, J.; Cotte, M.; Falkenberg, G.; et al. The Use of Synchrotron Radiation for the Characterization of Artists’ Pigments and Paintings. *Annu. Rev. Anal. Chem.* **2013**, *6*, 399–425. [\[CrossRef\]](#)
46. Pereira, M.O.; Felix, V.S.; Oliveira, A.L.; Ferreira, D.S.; Pimenta, A.R.; Carvalho, C.S.; Silva, F.L.; Perez, C.A.; Galante, D.; Freitas, R.P. Investigating counterfeiting of an artwork by XRF, SEM-EDS, FTIR and synchrotron radiation induced MA-XRF at LNLS-BRAZIL. *Spectrochim. Acta Part A Mol. Biomol. Spectrosc.* **2021**, *246*, 118925. [\[CrossRef\]](#) [\[PubMed\]](#)
47. Alberti, R.; Frizzi, T.; Bombelli, L.; Gironda, M.; Aresi, N.; Rosi, F.; Miliani, C.; Tranquilli, G.; Talarico, F.; Cartechini, L. CRONO: A fast and reconfigurable macro X-ray fluorescence scanner for in-situ investigations of polychrome surfaces. *X-ray Spectrom.* **2017**, *46*, 297–302. [\[CrossRef\]](#)
48. Freitas, R.P.; Felix, V.S.; Pereira, M.O.; Santos, R.S.; Oliveira, A.L.; Gonçalves, E.A.S.; Ferreira, D.S.; Pimenta, A.R.; Pereira, L.O.; Anjos, M.J. Micro-XRF analysis of a Brazilian polychrome sculpture. *Microchem. J.* **2019**, *149*, 104020. [\[CrossRef\]](#)

49. Alfeld, M.; Wahabzada, M.; Bauckhage, C.; Kersting, K.; van der Snickt, G.; Noble, P.; Janssens, K.; Wellenreuther, G.; Falkenberg, G. Simplex Volume Maximization (SiVM): A matrix factorization algorithm with non-negative constraints and low computing demands for the interpretation of full spectral X-ray fluorescence imaging data. *Microchem. J.* **2017**, *132*, 179–184. [\[CrossRef\]](#)
50. Lins, S.A.B.; Manso, M.; Lins, P.A.B.; Brunetti, A.; Sodo, A.; Gigante, G.E.; Fabbri, A.; Branchini, P.; Tortora, L.; Ridolfi, S. Modular MA-XRF Scanner Development in the Multi-Analytical Characterisation of a 17th Century Azulejo from Portugal. *Sensors* **2021**, *21*, 1913. [\[CrossRef\]](#)
51. Alfeld, M.; Laurenze-Landsberg, C.; Denker, A.; Janssens, K.; Noble, P. Neutron activation autoradiography and scanning macro-XRF of Rembrandt van Rijn's Susanna and the Elders (Gemäldegalerie Berlin): A comparison of two methods for imaging of historical paintings with elemental contrast. *Appl. Phys. A* **2015**, *119*, 795–805. [\[CrossRef\]](#)
52. Calza, C.; Oliveira, D.F.; de Souza Rocha, H.; Pedreira, A.; Lopes, R.T. Analysis of the painting "Gioventù" (Eliseu Visconti) using EDXRF and computed radiography. *Appl. Radiat. Isot.* **2010**, *68*, 861–865. [\[CrossRef\]](#)
53. De Campos, P.H.O.V. Caracterização de Pinturas da Artista Anita Malfatti Por Meio de Técnicas não Destrutivas. Ph.D. Thesis, Universidade de São Paulo, São Paulo, Brazil, 2015. [\[CrossRef\]](#)
54. Calza, C.; Pereira, M.O.; Pedreira, A.; Lopes, R.T. Characterization of Brazilian artists' palette from the XIX century using EDXRF portable system. *Appl. Radiat. Isot.* **2010**, *68*, 866–870. [\[CrossRef\]](#)
55. Solé, V.A.; Papillon, E.; Cotte, M.; Walter, P.; Susini, J. A multiplatform code for the analysis of energy-dispersive X-ray fluorescence spectra. *Spectrochim. Acta Part B At. Spectrosc.* **2007**, *62*, 63–68. [\[CrossRef\]](#)
56. Alfeld, M.; Janssens, K. Strategies for processing mega-pixel X-ray fluorescence hyperspectral data: A case study on a version of Caravaggio's painting Supper at Emmaus. *J. Anal. At. Spectrom.* **2015**, *30*, 777–789. [\[CrossRef\]](#)
57. Gonzalez, V.; Calligaro, T.; Wallez, G.; Eveno, M.; Toussaint, K.; Menu, M. Composition and microstructure of the lead white pigment in Masters paintings using HR Synchrotron XRD. *Microchem. J.* **2016**, *125*, 43–49. [\[CrossRef\]](#)
58. Lins, S.A.B.; Gigante, G.E.; Cesareo, R.; Ridolfi, S.; Brunetti, A. Testing the accuracy of the calculation of gold leaf thickness by mc simulations and MA-XRF scanning. *Appl. Sci.* **2020**, *10*, 3582. [\[CrossRef\]](#)
59. Cesareo, R.; de Assis, J.T.; Roldán, C.; Bustamante, A.D.; Brunetti, A.; Schiavon, N. Multilayered samples reconstructed by measuring $K\alpha/K\beta$ or $L\alpha/L\beta$ X-ray intensity ratios by EDXRF. *Nucl. Instrum. Methods Phys. Res. Sect. B Beam Interact. Mater. Atoms* **2013**, *312*, 15–22. [\[CrossRef\]](#)
60. Cesareo, R.; Brunetti, A.; Ridolfi, S. Pigment layers and precious metal sheets by energy-dispersive x-ray fluorescence analysis. *X-ray Spectrom.* **2008**, *37*, 309–316. [\[CrossRef\]](#)
61. Pessanha, S.; Queral, I.; Carvalho, M.L.; Sampaio, J.M. Determination of gold leaf thickness using X-ray fluorescence spectrometry: Accuracy comparison using analytical methodology and Monte Carlo simulations. *Appl. Radiat. Isot.* **2019**, *152*, 6–10. [\[CrossRef\]](#)
62. Lopes, F.; Melquiades, F.L.; Appoloni, C.R.; Cesareo, R.; Rizzutto, M.; Silva, T.F. Thickness determination of gold layer on pre-Columbian objects and a gilding frame, combining pXRF and PLS regression. *X-ray Spectrom.* **2016**, *45*, 344–351. [\[CrossRef\]](#)
63. Cesareo, R.; Ridolfi, S.; Brunetti, A.; Lopes, R.T.; Gigante, G.E. First results on the use of a EDXRF scanner for 3D imaging of paintings. *Acta IMEKO* **2018**, *7*, 8. [\[CrossRef\]](#)
64. Dik, J.; Janssens, K.; Van Der Snickt, G.; van der Loeff, L.; Rickers, K.; Cotte, M. Visualization of a Lost Painting by Vincent van Gogh Using Synchrotron Radiation Based X-ray Fluorescence Elemental Mapping. *Anal. Chem.* **2008**, *80*, 6436–6442. [\[CrossRef\]](#)
65. Alfeld, M.; Snickt, G.; Vanmeert, F.; Janssens, K.; Dik, J.; Appel, K.; Loeff, L.; Chavannes, M.; Meedendorp, T.; Hendriks, E. Scanning XRF investigation of a Flower Still Life and its underlying composition from the collection of the Kröller-Müller Museum. *Appl. Phys. A* **2013**, *111*, 165–175. [\[CrossRef\]](#)
66. Bell, I.M.; Clark, R.J.H.; Gibbs, P.J. Raman spectroscopic library of natural and synthetic pigments (pre- \approx 1850 AD). *Spectrochim. Acta Part A Mol. Biomol. Spectrosc.* **1997**, *53*, 2159–2179. [\[CrossRef\]](#)
67. Barnett, J.R.; Miller, S.; Pearce, E. Colour and art: A brief history of pigments. *Opt. Laser Technol.* **2006**, *38*, 445–453. [\[CrossRef\]](#)
68. Perez-Rodriguez, J.L.; de Haro, M.d.C.J.; Siguenza, B.; Martinez-Blanes, J.M. Green pigments of Roman mural paintings from Seville Alcazar. *Appl. Clay Sci.* **2015**, *116–117*, 211–219. [\[CrossRef\]](#)
69. Jorge-Villar, S.E.; Edwards, H.G.M. Green and blue pigments in Roman wall paintings: A challenge for Raman spectroscopy. *J. Raman Spectrosc.* **2021**, *52*, 2190–2203. [\[CrossRef\]](#)
70. Cucci, C.; Picollo, M.; Chiarantini, L.; Uda, G.; Fiori, L.; De Nigris, B.; Osanna, M. Remote-sensing hyperspectral imaging for applications in archaeological areas: Non-invasive investigations on wall paintings and on mural inscriptions in the Pompeii site. *Microchem. J.* **2020**, *158*, 105082. [\[CrossRef\]](#)
71. Eremin, K.; Stenger, J.; Huang, J.-F.; Aspuru-Guzik, A.; Betley, T.; Vogt, L.; Kassal, I.; Speakman, S.; Khandekar, N. Examination of pigments on Thai manuscripts: The first identification of copper citrate. *J. Raman Spectrosc.* **2008**, *39*, 1057–1065. [\[CrossRef\]](#)
72. Franquelo, M.L.; Perez-Rodriguez, J.L. A new approach to the determination of the synthetic or natural origin of red pigments through spectroscopic analysis. *Spectrochim. Acta Part A Mol. Biomol. Spectrosc.* **2016**, *166*, 103–111. [\[CrossRef\]](#)
73. Yu, J.; Warren, W.S.; Fischer, M.C. Visualization of vermilion degradation using pump-probe microscopy. *Sci. Adv.* **2019**, *5*, eaaw3136. [\[CrossRef\]](#)
74. Miliani, C.; Monico, L.; Melo, M.J.; Fantacci, S.; Angelin, E.M.; Romani, A.; Janssens, K. Recent insights into the photochemistry of artists' pigments and dyes: Towards better understanding and prevention of colour change in works of art. *Angew. Chem.* **2018**, *130*, 7447–7457. [\[CrossRef\]](#)

75. Freitas, R.P.; Ribeiro, I.M.; Calza, C.; Oliveira, A.L.; Silva, M.L.; Felix, V.S.; Ferreira, D.S.; Coelho, F.A.; Gaspar, M.D.; Pimenta, A.R.; et al. Analysis of clay smoking pipes from archeological sites in the region of the Guanabara Bay (Rio de Janeiro, Brazil) by FT-IR. *Spectrochim. Acta Part A Mol. Biomol. Spectrosc.* **2016**, *163*, 140–144. [[CrossRef](#)] [[PubMed](#)]
76. Vermeulen, M.; McGeachy, A.; Xu, B.; Chopp, H.; Katsaggelos, A.; Meyers, R.; Alfeld, M.; Walton, M. XRFast a new software package for processing of MA-XRF datasets using machine learning. *J. Anal. At. Spectrom.* **2022**, *37*, 2130–2143. [[CrossRef](#)]
77. Silva, T.F.; Trindade, G.F.; Rizzutto, M.A. Multivariate analysis applied to particle-induced X-ray emission mapping. *X-ray Spectrom.* **2018**, *47*, 372–381. [[CrossRef](#)]
78. Ferreira, E.S.B.; Gros, D.; Wyss, K.; Scherrer, N.C.; Zumbühl, S.; Marone, F. Faded shine The degradation of brass powder in two nineteenth century paintings. *Herit. Sci.* **2015**, *3*, 24. [[CrossRef](#)]

Disclaimer/Publisher’s Note: The statements, opinions and data contained in all publications are solely those of the individual author(s) and contributor(s) and not of MDPI and/or the editor(s). MDPI and/or the editor(s) disclaim responsibility for any injury to people or property resulting from any ideas, methods, instructions or products referred to in the content.